Journal of Radioanalytical and Nuclear Chemistry (2019) 322:553–559
https://doi.org/10.1007/s10967-019-06725-0

Adsorption of Th(IV) from aqueous solution by the graphene oxide nanoribbons/chitosan composite material

Peng Wu[2] · Yun Wang[1,2] · Yang Li[2] · Xuewen Hu[2] · Taoyuan Xiu[2] · Dingzhong Yuan[1] · Yan Liu[1] · Zhenyu Wu[3] · Zhirong Liu[1]

Received: 20 May 2019 / Published online: 28 August 2019

Abstract
In order to reduce the potential toxicity to the environment after treatment of radioactive waste water, an eco-friendly graphene oxide nanoribbons/chitosan (GONRs-CTS) composite was prepared and utilized for adsorption of Th(IV) from aqueous solution. The GONRs-CTS adsorbent was characterized by XRD, FTIR and SEM, indicating that GONRs-CTS contains a large amount of oxygen-containing groups and chitosan was successfully attached to the GONRs surface. The Th(IV) adsorption on GONRs-CTS was endothermic and spontaneous, with the maximum single layer adsorption capacity was 140.6 mg g^{-1} at pH = 3.0, in the contact time of 12 h. The adsorption process was consistent with pseudo-second-order kinetics and the Langmuir isotherm model.

Keywords Graphene oxide nanoribbons · Chitosan · Th(IV) · Adsorption

Introduction

In recent years, nuclear power generation, as an economical, efficient and clean energy source, is rapidly developing around the world [1]. Thorium is three to four times more abundant than uranium in nature [2], which can be used as a source of secondary nuclear fuel. A large number of wastewater with chemical and radiotoxicity is produced with the use of nuclear energy [3, 4]. Exposure to these radionuclides will bring about radiation hazards to the surrounding environment and human health. Therefore, from the perspective of the development and utilization of thorium resources, environmental protection and human health, it is urgent to study the high-efficiency separation and enrichment of thorium in aqueous solution.

In the past several decades, many adsorption media have been studied to separate, enrich and recover thorium. At present, the adsorption media used to separate and enrich thorium mainly include carbon materials, silicon materials, polymers, magnetic materials and biomass [5–10]. Nanometer-wide ribbons of graphene, namely graphene nanoribbons (GNRs), are a new favorite in the field of carbon nanomaterials in recent years. Its unique structure and a series of excellent properties have stimulated the research enthusiasm of researchers. GNRs are easier to adjust and have higher application value than graphene, and have excellent properties of both carbon nanotubes (CNTs) and graphene [11]. The oxidative chemical unzipping of multi-walled carbon nanotubes (MWCNTs) developed by Tour's team, providing a unique way for mass production of GNRs, these nanoribbons are called GONRs [12]. Besides, nanomaterials have potential toxicity in the ecological environment due to their difficulty in solid-liquid phase separation after practical application. Therefore, the practical application of nanodispersed GONRs in wastewater purification may be limited.

Chitosan is a non-toxic, bioactivity, bio-affinity and biodegradable polysaccharide [13]. Chitosan can form metal complexes with a variety of metal ions because of its molecular chain structure containing a large number of unpaired electron active groups (–NH_2, –OH). There are attractive prospects in applications such as wastewater treatment and metal catalysts [14–16]. In this work, an eco-friendly GONRs-CTS composite was synthesized, which reduced the

✉ Yun Wang
lovecit@163.com

[1] State Key Laboratory of Nuclear Resources and Environment, East China University of Technology, Nanchang 330013, China

[2] School of Nuclear Science and Engineering, East China University of Technology, Nanchang 330013, China

[3] China Institute of Atomic Energy, Beijing 102413, China

potential toxicity of nanomaterials in the environment. Then, the adsorption efficiency of thorium in aqueous solution by GONRs-CTS was investigated under the influence of various experimental parameters.

Experimental

Materials

All chemicals were of AR grade, which include H_2SO_4 (98%), $KMnO_4$, Chitosan, H_2O_2 (30%), epichlorohydrin and ethanol. Their chemicals were purchased from Xilong Scientific Co., Ltd. (China). MWCNTs (The purity of 95%) were purchased from Chengdu organic chemicals Co., Ltd. (China). The Th(IV) stock solutions (1000 mg L^{-1}) were prepared from $Th(NO_3)_4{\cdot}4H_2O$ (AR, Aladdin) after dissolution and dilution with deionized water. The stock solution was diluted to prepare working solutions as required.

Instrumentation

Th(IV) as Th(IV)-arsenazo(III) complex at 660 nm were determined by UV–spectrophotometer (721-type spectrophotometer). The structure and morphologies of GONRs and GONRs-CTS were identified using SEM (Model: FEI Nova NanoSEM450) at the accelerating voltage of 5.0 kV. Fourier transform infrared (FTIR) spectra were recorded on a IR-843 spectrophotometer using KBr disc. The X-ray diffraction pattern of the materials were recorded by X-ray powder diffraction (D8 advance) diffractometer and samples were scanned from 5° to 40° (2θ).

Synthesis of GONRs

Synthetic procedure of GONRs was the same to our previous paper [17].

Synthesis of GONRs-CTS composites

Chitosan (1 g) was dissolved entirely in glacial acetic acid (1%, 100 mL) and stirred magnetically at 45 °C for 2 h. Then the pH was adjusted to 5 with of NaOH (0.1 mol L^{-1}). GONRs (1 g) was added to 100 mL deionized water for ultrasonic treatment for 30 min and the suspension was formed by magnetic stirring at 60 °C for 30 min. The chitosan solution and GONRs solution were mixed at a ratio of 5:1 and stirred at 60 °C for 4 h. The above mixed solution was uniformly coated in a culture dish and dried in an oven at 60 °C for 5 h to form film. The film was immersed in a 5% ethanol solution of epichlorohydrin and dried at 60 °C for 20 h. The film was washed several times with deionized water and dried overnight. The solid product was denoted as GONRs-CTS.

Adsorption experiments

The adsorption behavior of GONRs-CTS for Th(IV) was investigated by batch mode experiments. The effects of different parameters such as pH, contact time, initial Th(IV) concentration, temperature and adsorbent dosage were examined. The adsorption mechanism was studied using kinetics, adsorption isotherms and thermodynamic models. GONRs-CTS (0.005–0.045 g) was weighed and transferred into a 50 mL glass vials containing 20 mL Th(IV) solution (25 mg L^{-1}). The pH of the thorium solutions was adjusted to be in the range of 1–7 by the addition of HNO_3 or NaOH solutions. Then, the mixture was shaken for different periods at room temperature to achieve an adsorption equilibrium. The GONRs-CTS adsorption capacity (q_e, mg g^{-1}) and removal efficiency (p, %) for Th(IV) were calculated by Eqs. (1) and (2), respectively.

$$q_e = \frac{C_0 - C_e}{m} \times V \tag{1}$$

$$p = \frac{C_0 - C_e}{C_0} \times 100\% \tag{2}$$

where C_0 and C_e (mg L^{-1}) represent the initial and equilibrium solution concentrations of Th(IV), respectively. m and V designate the weight (g) of the GONRs-CTS and the solution volume (L), respectively.

Results and discussion

Characterization of GONRs-CTS

The morphologies of GONRs and GONRs-CTS were observed by SEM, as shown in Fig. 1. The GONRs are nanometer-wide ribbons of graphene (Fig. 1a) [18]. The surface of GONRs-CTS is rough and have many folds, which may be due to the effect of CTS on overlapping the GONRs (Fig. 1b, c).

The main groups on the surface of GONRs, CTS and GONRs-CTS composites were determined by FT-IR analysis and the results are presented in Fig. 2. The FT-IR spectrum of GONRs displays the characteristic peaks at 3460 cm^{-1} (–OH vibrations), 2930 and 2860 cm^{-1} (C–H vibrations), 1610 cm^{-1} (C=O vibrations), 1053 cm^{-1} (C–O vibrations) [19]. As previously reported [20], the FT-IR spectra of CTS showed the characteristic peaks at 3435 cm^{-1} (–OH and –NH vibrations), 2920 and 2863 cm^{-1} (–CH and $–CH_2$ vibrations), 1605 cm^{-1} (–NH

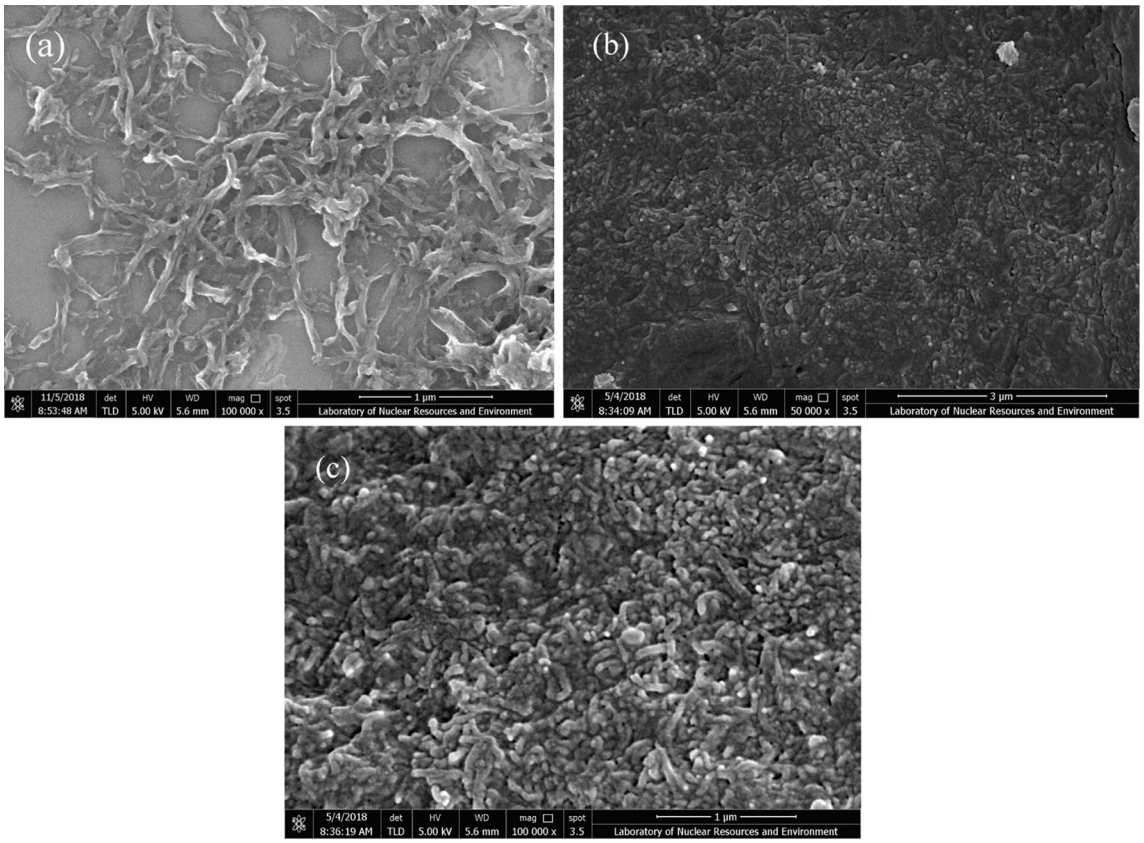

Fig. 1 SEM images of GONRs (**a**), GONRs-CTS (**b**, **c**)

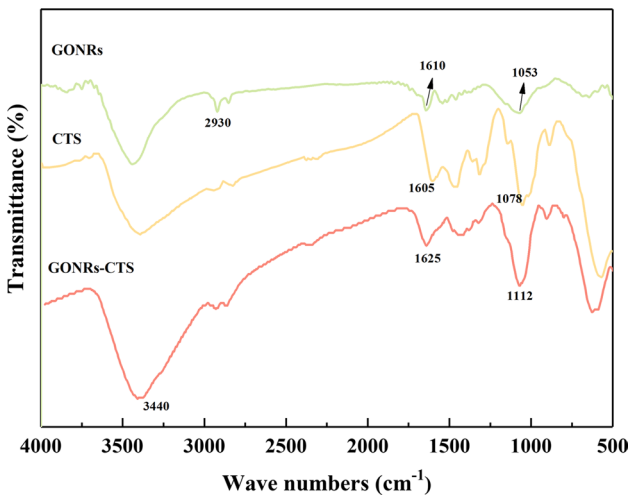

Fig. 2 FTIR spectra of GONRs, CTS and GONRs-CTS

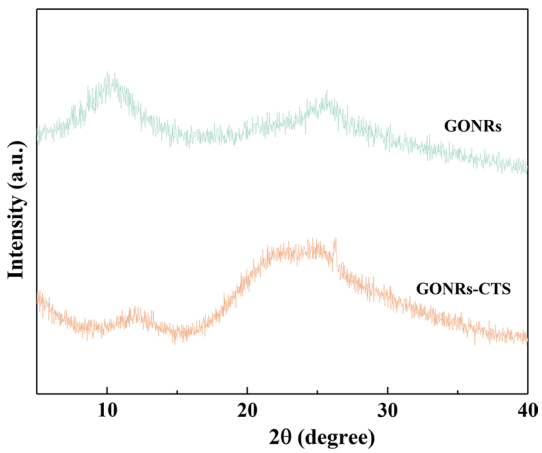

Fig. 3 XRD patterns of GONRs and GONRs-CTS

and –NH_2), 1420 and 1383 cm^{-1} (–CO), 1078 cm^{-1} (C–O vibrations). Finally, the FT-IR spectra of GONRs-CTS showed the characteristic peaks at 3440 cm^{-1} (–OH vibrations), 2943 and 2871 cm^{-1} (C–H), 1625 cm^{-1} (–NH vibrations), 1112 cm^{-1} (C–O) [21].

Figure 3 shows the XRD patterns of GONRs and GONRs-CTS. The specific 2θ peak of GONRs at 10.2° corresponds to (001). The (002) diffraction peak of graphite appears at $2\theta = 25.4°$, which was attributed to the MWCNTs not being wholly unzipped in the oxidizing environment [22]. The diffraction peaks of carbon nanomaterials are consistent with the standard card JCPDS #49-1721. In the case of

GONRs-CTS, the intense (001) peak decreased, while broad diffraction peaks appear between $2\theta = 21.7°–26.1°$, indicating that the chitosan is well compounded on the surface of the GONRs. It may be related to the amorphous state and crystal structure of chitosan [23].

Effect of pH on thorium adsorption onto GONRs-CTS

The pH of solution is a critical parameter affecting the sorption of thorium on adsorbent because it influences the species of thorium ions and the active sites of the sorbent in the solution. The adsorption of GONRs-CTS was investigated in the pH range of 1.0–7.0 (Fig. 4). As it could be seen clearly from Fig. 4, the adsorption capacity of Th(IV) increased sharply with an increase of pH from 1.0 to 5.0. When the pH increased beyond 5.0, the adsorption capacity remained constant. The adsorption capacity of Th(IV) is lower at pH value below 1.0–3.0 because the adsorbent surface was positively charged thus resulting in the competition between H^+ and Th^{4+} ions for the same adsorption site [24]. As the pH of the solution increases, the electrostatic repulsion of the GONRs-CTS surface disappears. However, thorium ions begin to hydrolyze into hydroxide complex [$Th(OH)^{3+}$, $Th(OH)_2^{2+}$, $Th(OH)_3^{+}$ and precipitation] at high pH value [25]. The initial pH was optimized to 3.0 in order to obtain high adsorption capacity and avoid precipitation of Th(IV).

Effect of the adsorbent dosage on adsorption

The effect of GONRs-CTS dosage (varied from 0.005 to 0.045 g) on Th(IV) adsorption was shown in Fig. 5. The Th(IV) adsorption capacity decreases as the amount of GONRs-CTS dosage was further increased. However, as the amount of adsorbent increases, the active site on the surface of the GONRs-CTS increases, and the adsorbent tends to be saturated. Therefore, the removal efficiency of Th(IV) from aqueous solution on GONRs-CTS increases. Hence, in order to maintain a balance between removal efficiency and adsorption capacity, 15 mg was optimized as the adsorbent dosage for all adsorption experiments.

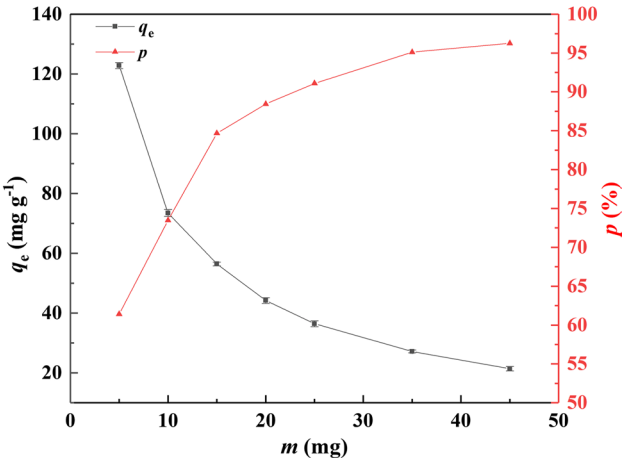

Fig. 5 Effect of adsorbent dosage on the thorium adsorption, pH = 3.0, $C_0 = 50$ mg L^{-1}, $V = 20$ mL, $t = 12$ h, and $T = 298.15$ K

Effect of contact time and kinetic studies

The effect of the contact time on the adsorption of Th(IV) onto GONRs-CTS is shown in Fig. 6. Experiments were performed to study the effect of the contact time on Th(IV) sorption on GONRs-CTS at different times varying from 10 to 1080 min. Figure 6 shows that as the contact time increases, the adsorption capacity of Th(IV) on GONRs-CTS increases rapidly and then tends to equilibrium. The adsorption was initially fast and then reached equilibrium within 12 h and the removal

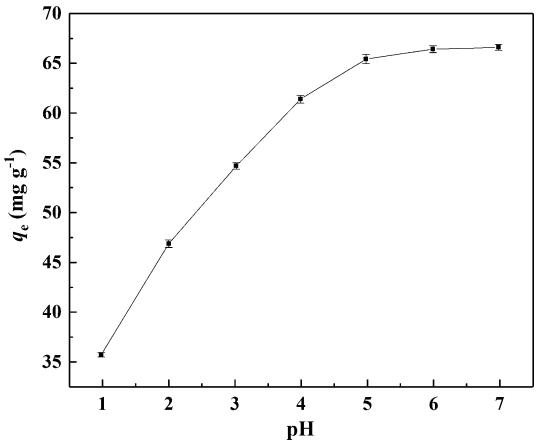

Fig. 4 Effect of pH on the adsorption of thorium onto GONRs-CTS, $m = 15$ mg, $C_0 = 50$ mg L^{-1}, $V = 20$ mL, $t = 12$ h, and $T = 298.15$ K

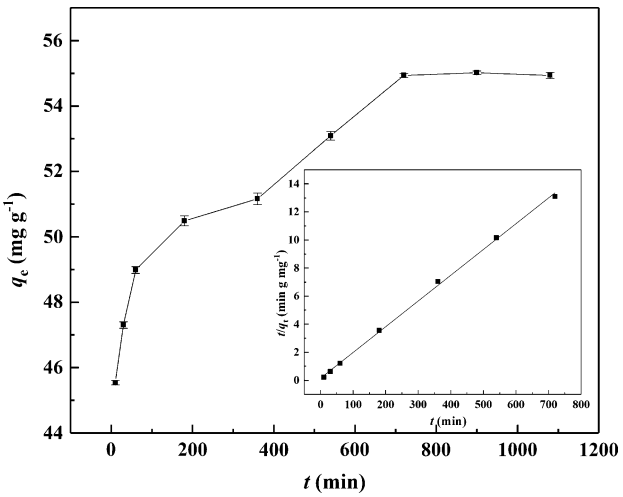

Fig. 6 Effect of contact time on the thorium adsorption, pH = 3.0, $C_0 = 50$ mg L^{-1}, $V = 20$ mL, $m = 15$ mg, and $T = 298.15$ K

efficiency at equilibrium was 82.4%. Therefore, 12 h was selected from the above results as the optimum contact time.

Adsorption kinetics is an important aspect of determining the efficiency of the adsorption process. The pseudo-first-order and pseudo-second-order were employed to describe the kinetic characteristics of the sorption of Th(IV) on GONRS-CTS. The kinetic models can be expressed as the following Eqs. (3) and (4).

$$\ln\left(q_e - q_t\right) = \ln q_e - k_1 t \tag{3}$$

$$\frac{t}{q_t} = \frac{1}{k_2 q_e^2} + \frac{t}{q_e} \tag{4}$$

where q_e and q_t (mg g^{-1}) are the amounts of Th(IV) ions adsorbed of GONRs-CTS at equilibrium and at any time t, respectively. k_1 (min^{-1}) and k_2 (g mg^{-1} min^{-1}) are the adsorption rate the constants of pseudo-first-order and pseudo-second-order, respectively.

Kinetic parameters are calculated and shown in Table 1 and Fig. 6. The theoretical value of the adsorption capacity was calculated from the slope and intercept of the fitted curve. The highest correlation coefficient value of pseudo-second-order model ($R^2 = 0.9988$) and the closest $q_{e,cal}$ (55.30 mg g^{-1}) to $q_{e,exp}$ (54.94 mg g^{-1}) show the second-order nature of the present sorption process.

Adsorption isotherm

The adsorption properties of the adsorbent are described by adsorption isotherms which is plots of adsorption capacity (q_e) and final equilibrium solute concentration (C_e). Therefore, experimental data were evaluated by both Langmuir isotherm and Freundlich isotherm models (Fig. 7). The Langmuir adsorption isotherm assumes that the adsorbed molecules form an adsorption layer of one molecule in thickness and all sites are equal, resulting in equal energy and adsorption enthalpy. The Freundlich adsorption isotherm is obtained by assuming a non-uniform surface with a non-uniform adsorption heat distribution on the surface. The linear equations of the Langmuir and Freundlich isotherm models can be respectively expressed as

$$\frac{C_e}{q_e} = \frac{1}{q_m K_L} + \frac{C_e}{q_m} \tag{5}$$

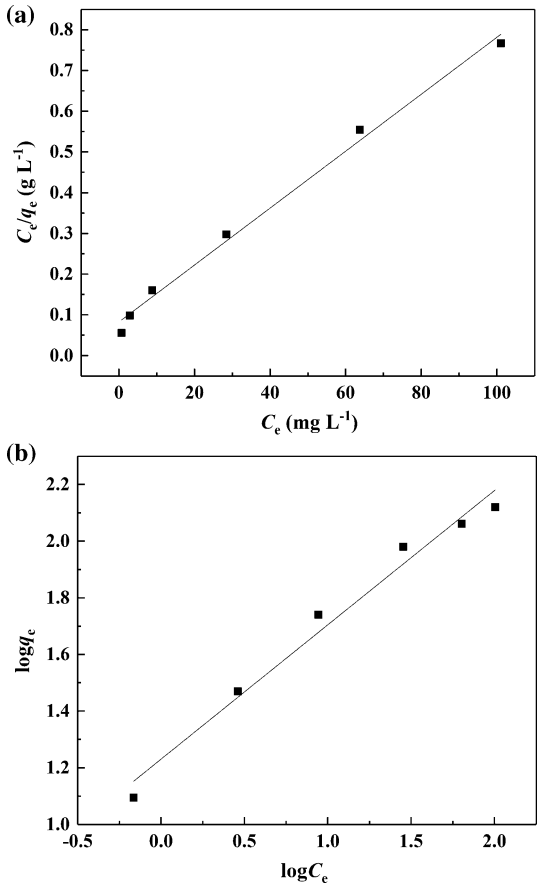

Fig. 7 Langmuir (**a**) and Freundlich (**b**) isotherm plot of thorium adsorption for GONRs-CTS

$$\log q_e = \log K_F + \frac{1}{n}\log C_e \tag{6}$$

where C_e (mg L^{-1}) is the equilibrium concentration, q_e (mg g^{-1}) is the amounts of Th(IV) adsorbed per gram of sorbent at equilibrium, q_m (mg g^{-1}) and K_L (L mg^{-1}) are the Langmuir constants associated with adsorption capacity and adsorption energy, respectively. K_F ($mg^{1-1/n}$ $L^{1/n}$ g^{-1}) and n are the Freundlich characteristic constants representing adsorption capacity and adsorption intensity respectively.

The parameters for the isotherm models are listed in Table 2. As can be seen, the values of R^2 show that the Langmuir ($R^2 = 0.9930$) model can describe the experimental data better than the Freundlich ($R^2 = 0.9804$). This indicates that

Table 1 Kinetic parameters for the adsorption

Pseudo-first-order			Pseudo-second-order		
$q_{e,cal}$ (mg g^{-1})	k_1 (min^{-1})	R^2	$q_{e,cal}$ (mg g^{-1})	k_2 (g mg^{-1} min^{-1})	R^2
8.046	0.0028	0.9381	55.30	0.0020	0.9988

Table 2 The isothermal adsorption model parameters

Langmuir			Freundlich		
q_m (mg g^{-1})	K_L (L mg^{-1})	R^2	K_F ($mg^{1-1/n}$ $L^{1/n}$ g^{-1})	n	R^2
140.6	0.0847	0.9930	16.99	2.109	0.9804

the adsorption process of Th(IV) in GONRs-CTS is monolayer adsorption.

Another basic feature of the Langmuir model can be described by the separation factor (R_L). The separation factor can be expressed as the following Eqs. (7).

$$R_L = \frac{1}{\left(1 + K_L C_0\right)} \tag{7}$$

The separation factor calculated according to K_L which gave an indication for the possibility of the adsorption process to proceed as follows: $R_L > 1$ is an unfavorable process; $R_L = 1$ is a linear process; $R_L < 1$ shows favorable adsorption [26]. The values of R_L lie between 0.5414 and 0.0557, indicating that Th(IV) from aqueous solution adsorbent on GONRS-CTS is favorable.

Adsorption thermodynamics

The adsorption thermodynamics is very important to understand the adsorption mechanism of Th(IV) on the adsorbent. The values of $\Delta H°$ and $\Delta S°$ listed in Table 3 were calculated from the slope and intercept of the plots of ln K_d versus T^{-1} (Fig. 8). The thermodynamic parameters such as the Gibbs free energy ($\Delta G°$), enthalpy ($\Delta H°$), and entropy ($\Delta S°$) can be calculated by the following Eqs:

$$K_d = \frac{C_0 - C_e}{C_e} \times \frac{V}{m} \tag{8}$$

$$\ln K_d = \frac{\Delta S^o}{R} - \frac{\Delta H^o}{RT} \tag{9}$$

$$\Delta G^o = \Delta H^o - T\Delta S^o \tag{10}$$

where K_d (mL g^{-1}) is the distribution coefficient, T (K) and R (8.314 J mol^{-1} K^{-1}) are the absolute temperature in Kelvin and the gas constant.

As shown in Table 3, the negative values of $\Delta G°$ increased with increasing temperature and the absolute value increases, indicating that the adsorption process was spontaneous and irreversible. The positive value of $\Delta H°$ (23.06 kJ mol^{-1}) confirmed that the adsorption process was an endothermic reaction, and the adsorption process was more favorable at higher temperatures. At the same time, the positive values of $\Delta S°$ (150.60 J mol^{-1} K^{-1}) suggested an increase in the degree of freedom of the solid-solution interface during the adsorption process.

Table 3 Thermodynamic parameters of thorium adsorption on MGONRs

$\Delta S°$ (J mol^{-1} K^{-1})	$\Delta H°$ (kJ mol^{-1})	$\Delta G°$ (kJ mol^{-1})		
		298 K	308 K	318 K
150.60	23.06	−21.82	−23.33	−24.84

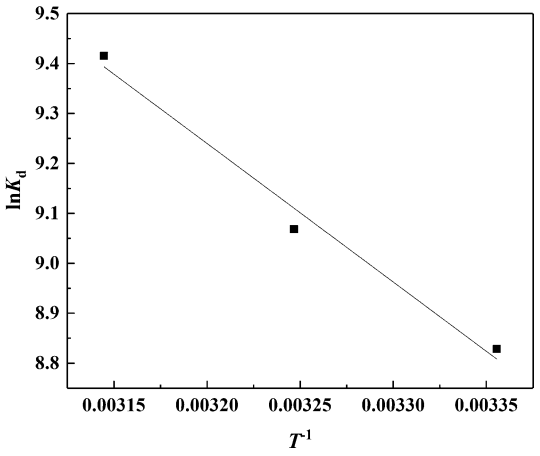

Fig. 8 The adsorption thermodynamics of Th(IV) on GONRs-CTS, pH = 3.0, C_0 = 50 mg L^{-1}, V = 20 mL, t = 12 h, and m = 15 mg

Effect of coexisting anions

Figure 9 shows the effect of coexisting anions on the adsorption of Th(IV) from aqueous solutions onto GONRs-CTS. The addition of Cl^- had no effect on the adsorption of Th(IV) on GONRs-CTS. CO_3^{2-} and HCO_3^- has a coordination exchange on the surface of GONRs-CTS, which increases the negative charge and adsorption sites on the surface and promotes the adsorption of Th(IV) on GONRs-CTS. Under acidic conditions, SO_4^{2-} and HSO_4^- forms a complex with Th^{4+}, which leads to an increase in Th^{4+} in solution and a decrease in Th^{4+} on the surface of GONRs-CTS.

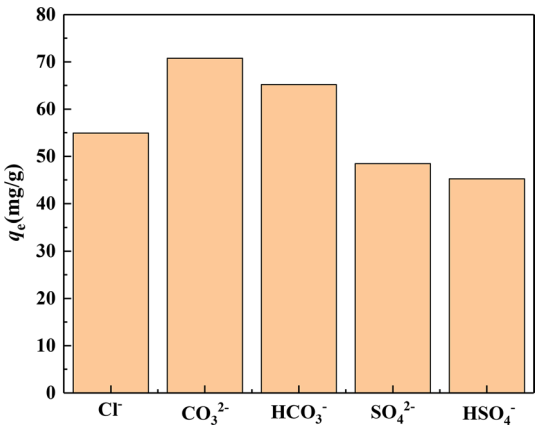

Fig. 9 Effect of coexisting anions(0.01 M) on adsorption of Th(IV)

Conclusion

The batch adsorption results show that GONRs-CTS composite material has excellent adsorption performance of thorium from aqueous solution. Thorium adsorption on the GONRs-CTS was a pH dependent, spontaneous, endothermic and a pseudo-second-order process. The maximum adsorption capacity calculated by Langmuir isotherm equation was 140.6 mg g^{-1}. This eco-friendly GONRs-CTS sorbent is expected to be applied to thorium from radioactive waste water.

Acknowledgements This work was financially supported by the National Natural Science Foundation of China (21601033, 21866006, 11875105, 21661003, 11705027), and Jiangxi Province Key Subjects Academy and Technique Leaders Funding Project (20172BCB22020), Natural Science Funds for Distinguished Young Scholar of Jiangxi Province (20171BCB23067), Open Project Foundation of Nuclear Technology Application Ministry of Education Engineering Research Center (East China University of Technology) (HJSJYB2016-6), Open Project Foundation of Stake key Laboratory of Nuclear Resources and Environment (East China University of Technology) (NRE1509), the Fundamental Science on Nuclear Wastes and Environmental Safety Laboratory (No. 16kfhk02).

References

1. Liu Z, Liu D, Cai Z, Wang Y, Zhou L (2018) Synthesis of new type dipropyl imide chelating resin and its potential for uranium(VI) adsorption. J Radioanal Nucl Chem 318(2):1219–1227
2. Pan N, Li L, Ding J, Li S, Wang R, Jin Y, Wang X, Xia C (2016) Preparation of graphene oxide-manganese dioxide for highly efficient adsorption and separation of Th(IV)/U(VI). J Hazard Mater 309:107–115
3. Galhoum AA, Mahfouz MG, Atia AA, Abdel-Rehem ST, Gomaa NA, Vincent T, Guibal E (2015) Amino acid functionalized chitosan magnetic nanobased particles for uranyl sorption. Ind Eng Chem Res 54(49):12374–12385
4. Anirudhan TS, Radhakrishnan PG (2009) Improved performance of a biomaterial-based cation exchanger for the adsorption of uranium(VI) from water and nuclear industry wastewater. J Environ Radioact 100(3):250–257
5. Lu X, Zhang D, Tesfay Reda A, Liu C, Yang Z, Guo S, Xiao S, Ouyang Y (2017) Synthesis of amidoxime-grafted activated carbon fibers for efficient recovery of uranium(VI) from aqueous solution. Ind Eng Chem Res 56(41):11936–11947
6. Chen L, Zhao D, Chen S, Wang X, Chen C (2016) One-step fabrication of amino functionalized magnetic graphene oxide composite for uranium(VI) removal. J Colloid Interface Sci 472:99–107
7. He JD, Wang YD, Hu N, Ding D, Sun J, Deng QW, Li CW, Xu F (2015) An artificially constructed *Syngonium podophyllum–Aspergillus niger* combinate system for removal of uranium from wastewater. Environ Sci Pollut Res 22(23):18918–18926
8. Yuan D, Chen L, Xiong X, Yuan L, Liao S, Wang Y (2016) Removal of uranium (VI) from aqueous solution by amidoxime functionalized superparamagnetic polymer microspheres prepared by a controlled radical polymerization in the presence of DPE. Chem Eng J 285:358–367
9. Basu H, Singhal RK, Pimple MV, Manisha V, Bassan MKT, Reddy AVR, Mukherjee T (2011) Development of naturally occurring siliceous material for the preferential removal of thorium from U–Th from aquatic environment. J Radioanal Nucl Chem 289(1):231–237
10. Kaynar UH, Şabikoğlu İ (2018) Adsorption of thorium (IV) by amorphous silica; response surface modelling and optimization. J Radioanal Nucl Chem 318(2):823–834
11. Wang Y, Wang Z, Ran R, Yang J, Liu N, Liao J, Yang Y, Tang J (2015) Synthesis of amidoximated graphene oxide nanoribbons from unzipping of multiwalled carbon nanotubes for selective separation of uranium(VI). RSC Adv 5(108):89309–89318
12. Higginbotham AL, Kosynkin DV, Alexander S, Zhengzong S, Tour JM (2010) Lower-defect graphene oxide nanoribbons from multiwalled carbon nanotubes. ACS Nano 4(4):2059–2069
13. Vakili M, Rafatullah M, Salamatinia B, Abdullah AZ, Ibrahim MH, Tan KB, Gholami Z, Amouzgar P (2014) Application of chitosan and its derivatives as adsorbents for dye removal from water and wastewater: a review. Carbohydr Polym 113:115–130
14. Hsan N, Dutta PK, Kumar S, Bera R, Das N (2019) Chitosan grafted graphene oxide aerogel: synthesis, characterization and carbon dioxide capture study. Int J Biol Macromol 125:300–306
15. Fan L, Luo C, Sun M, Li X, Qiu H (2013) Highly selective adsorption of lead ions by water-dispersible magnetic chitosan/graphene oxide composites. Colloids Surf B Biointerfaces 103:523–529
16. Marques JS, Pereira MR, Sotto A, Arsuaga JM (2019) Removal of aqueous copper(II) by using crosslinked chitosan films. React Funct Polym 134:31–39
17. Wu P, Wang Y, Hu X, Yuan D, Liu Y, Liu Z (2018) Synthesis of magnetic graphene oxide nanoribbons composite for the removal of Th(IV) from aqueous solutions. J Radioanal Nucl Chem 319(3):1111–1118
18. Xiu T, Liu Z, Wang Y, Wu P, Du Y, Cai Z (2019) Thorium adsorption on graphene oxide nanoribbons/manganese dioxide composite material. J Radioanal Nucl Chem 319(3):1059–1067
19. Omidi S, Kakanejadifard A (2018) Eco-friendly synthesis of graphene–chitosan composite hydrogel as efficient adsorbent for Congo red. RSC Adv 8(22):12179–12189
20. Reddy DH, Lee SM (2013) Application of magnetic chitosan composites for the removal of toxic metal and dyes from aqueous solutions. Adv Colloid Interface Sci 201–202:68–93
21. Samuel MS, Bhattacharya J, Raj S, Santhanam N, Singh H, Pradeep Singh ND (2019) Efficient removal of Chromium(VI) from aqueous solution using chitosan grafted graphene oxide (CS-GO) nanocomposite. Int J Biol Macromol 121:285–292
22. Wang Y, Wang Z, Gu Z, Yang J, Liao J, Yang Y, Liu N, Tang J (2015) Uranium(VI) sorption on graphene oxide nanoribbons derived from unzipping of multiwalled carbon nanotubes. J Radioanal Nucl Chem 304(3):1–9
23. Huang Z, Li Z, Zheng L, Zhou L, Chai Z, Wang X, Shi W (2017) Interaction mechanism of uranium(VI) with three-dimensional graphene oxide-chitosan composite: insights from batch experiments, IR, XPS, and EXAFS spectroscopy. Chem Eng J 328:1066–1074
24. Shehzad H, Zhou L, Li Z, Chen Q, Wang Y, Liu Z, Adesina AA (2017) Effective adsorption of U(VI) from aqueous solution using magnetic chitosan nanoparticles grafted with maleic anhydride: equilibrium, kinetic and thermodynamic studies. J Radioanal Nucl Chem 315(2):195–206
25. Bozkurt SS, Molu ZB, Cavas L, Merdivan M (2011) Biosorption of uranium (VI) and thorium (IV) onto Ulva gigantea (Kützing) bliding: discussion of adsorption isotherms, kinetics and thermodynamic. J Radioanal Nucl Chem 288(3):867–874
26. Gado MA (2018) Sorption of thorium using magnetic graphene oxide polypyrrole composite synthesized from natural source. Sep Sci Technol 53(13):2016–2033